New Radiating Edges-Coupling (REC) Model for the Gap Between Two Rectangular Microstrip Patch Antennas

(구형 마이크로스트립 안테나의 간격에 대한 새로운 Radiating Edges-Coupling(REC) 모델)

洪 在 杓,* 趙 榮 基,* 孫 鉉*

(Jae Pyo Hong, Young Ki Cho and Hyon Son)

要 約

본 논문에서는 결합된 구형 마이크로스트립 안테나사이의 간격에 대한 새로운 등가모델인 Radiating Edges-Coupling(REC) 모델을 제시하였다. REC모델은 균일한 유전체로 채워져 있고 윗면에 슬릿이 있는 평행평판 도파로의 등가회로로 부터 유도하였다. 결합간격이 0.5, 1.0, 1.5, 및 2.0mm인 경우에 REC모델을 적용하여 2.5GHz와 3.5GHz 사이의 주파수에서 산란계수 $|S_{11}|$과 $|S_{12}|$의 이론치와 실험치를 비교한 결과 서로 일치되는 양호한 특성을 얻었다.

Abstract

In this paper, a new model is presented which characterizs the coupling of the radiating edges between two rectangular microstrip patch antennas. This model, namely Radiating Edges-Coupling (REC) model, is derived from the equivalent circuit of the slitted parallel-plate waveguide filled with homogeneous dielectric. Applying the REC model to two coupled rectangular microstrip patch antennas, we obtain numerical S-parameter values of $|S_{11}|$ and $|S_{12}|$ for the various coupling separations, S_e=0.5, 1.0, 1.5, and 2.0mm. Theoretical results are in fairly good agreement with experimental results.

I. Introduction

Experimental papers for increasing the bandwidth of the rectangular microstrip patch antennas by use of the coupling in the radiating edges of a rectangular patch have been reported[1]-[5].

Maeda[6] modeled the gap in microstrip lines as an equivalent circuit with a series gap capacitance and two shunt gap capacitances. These capacitances are formulated with three-dimensional Green's function, based on a variational principle. Applying the equivalent circuit to the gap between two microstrip patches, Krowne [7],[8] proposed initially a model (E-plane coupling model) which accounts for the coupling of the radiating edges between two rectangular microstrip patch antennas. Also, a method for

*正會員, 慶北大學校 電子工學科

(Dept. of Elec. Eng., Kyungpook Nat'l Univ.)

接受日字：1988年 9月 13日

increasing the bandwidth of microstrip patch antenna by use of two parasitic elements which are coupled to the radiating edges of a rectangular patch antenna has been experimentally investigated by Kumar and Gupta[4],[5]. Lee et al.[9] obtained experimentally the increase in gain without degradation in radiation patterns by using the microstrip antennas which consist of one centre-fed and several identical parasitic patches. Recently, based on the experimental study, Özmehmet[10] proposed an equivalent model for the gap in microstrip lines as a multi-element circuit which has frequency dependent capacitances and a radiation conductance. However a theoretical model for the coupled gap has not been available so far.

In this paper, a new model, namely Radiating Edges-Coupling (REC) model, is presented which characterizes the coupling of the radiating edges between two rectangular microstrip patch antennas. The REC model is derived from the equivalent circuit[11]-[14] of the slitted parallel-plate waveguide filled with homogeneous dielectric.

For the four coupling separations, S_e=0.5, 1.0, 1.5, and 2.0 mm, numerical scattering parameter results of $|S_{11}|$ and $|S_{12}|$ are calculated in the frequency range of 2.5-3.5 GHz by the use of the REC model and the radiation admittance of a rectangular microstrip patch antenna given by Hong et al.[14]. The two rectangular microstrip patch antennas are fabricated in Teflon substrate with relative dielectric constant ϵ_r=2.6 and thickness h=0.155 cm. The theoretical and experimental results are compared with theoretical results obtained by the E-plane coupling model of Krowne[7].

II. New Radiating Edges-Coupling (REC) Model

The geometry of the slitted parallel-plate waveguide filled with homogeneous dielectric is shown in Fig.1(a). Here h is the waveguide height and 2a is the slit width.

When a TEM wave is incident upon the slit, the slitted parallel-plate waveguide shown in Fig.1(a) is represented by the equivalent circuit[11]-[14] shown in Fig.1(b). In Fig.1(b), the normalized series admittance $\bar{Y}_1$, shunt admittance $\bar{Y}_2$, and load admittance $\bar{Y}_L$ are expressed in tersm of the TEM magnetic field reflection and transmission coefficients[11]-[14].

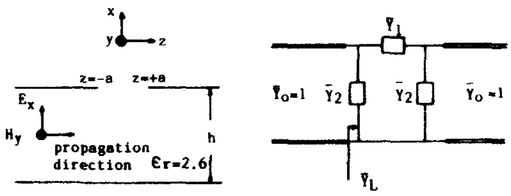

(a) (b)

Fig.1. (a) Geometry of a parallel-plate waveguide filled with homogenous dielectric.
(b) Equivalent circuit

In Fig.1(b), for the case of Ka<0.2, i.e., the narrow slit width, the significant results are found as follows: Here K is the propagation constant of the free space.

1) The normalized series admittance $\bar{Y}_1 = \bar{G}_1 + j\bar{B}_1$:

The normalized series conductance G_1 is nearly constant and the same as the normalized load conductance $\bar{G}_L$ for the case of Ka>0.1. Furthermore, this normalized load conductance is identical to the normalized radiation conductance of a rectangular microstrip patch antenna given by Bahl[15]. The unnormalized series susceptance is represented by a capacitance because it is always positive. As the slit width narrows, the capacitance increases.

2) The normalized shunt admittance $\bar{Y}_2 = \bar{G}_2 + j\bar{B}_2$:

The normalized shunt conductance $\bar{G}_2$ is extremely small so that it can be neglected. Also the unnormalized shunt susceptance is represented by a capacitance because it is always positive. The capacitance decreases as the slit width narrows.

From the above results, when the slit width 2a is in the range of Ka< 0.2, the parameters of the equivalent circuit shown in Fig.1(b) are summarized as follows:

1) The series admittance consists of a parallel combination of a conductance which is equivalent to the radiation conductance of a rectangular microstrip patch antenna and a capacitance determined from the unnormalized series susceptance.
2) The shunt admittance consists of a capacitance determined from the unnormalized shunt susceptance.

The geometry of gap between two coupled rectangular microstrip patch antennas is shown in Fig.2(a). Here, S_e is the coupling separation between the radiating edges. h is the substrate thickness. As discussed in [11], the results of the two dimensional analysis are valid for microstrip radiating patch application. Therefore the equivalent circuit parameters which characterize the coupling of the radiating edges between two rectangular microstrip patch antennas shown in Fig.2(a) can be derived from the equivalent circuit parameters of the slitted parallel-plate waveguide shown in Fig.1(b).

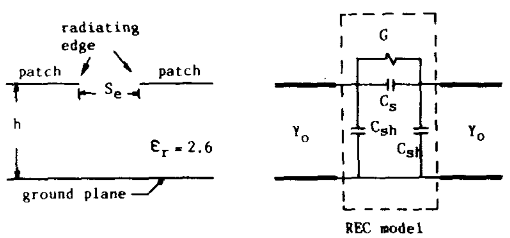

(a) (b)

Fig.2. (a) Geometry of gap between two coupled rectangular microstrip patch antennas.
(b) Radiating Edges-Coupling (REC) model.

Based on the above discussion, when the coupling separation S_e is the same as the slit width for Ka<0.2, the equivalent circuit model for the gap between two coupled rectangular microstrip patch antennas is shown in Fig.2(b). As seen in Fig.2(b), the equivalent model, namely Radiating Edges-Coupling (REC) model, which characterizes the coupling between the radiating edges consists of the radiation conductance G of a rectangular microstrip patch antenna given by Hong et al.[4] and the series and shunt capacitances (C_s and C_{sh}) determined from the series and shunt susceptances of the equivalent circuit given in [11], [12].

An equivalent circuit which is experimentally modeled for the gap discontinuity in microstrip lines by Özmehmet[10], was considerably similiar to the REC model which is theoretically presented in this paper.

III. Expressions for Scattering Parameters and Numerical Results

The geometry of two rectangular patch antennas which are coupled to the radiating edges between the patches is shown in Fig.3. Here, the rectangular microstrip patch antenna is fed by a coaxial line and this antenna is fed along the center of the patch width at the feed point location X. S_e is the coupling separation. W and L are the width and length of the antenna, respectively. h is the substrate thickness and ϵ_r is the relative dielectric constant.

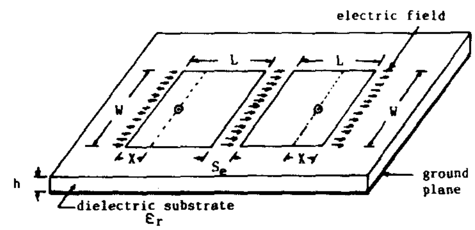

Fig.3. Geometry of two coupled rectangular microstrip patch antennas.

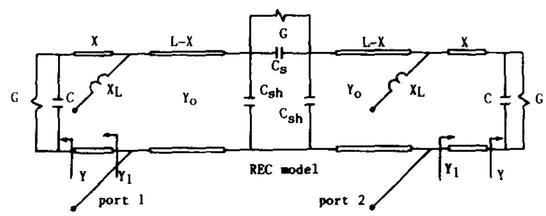

Fig.4. Equivalent circuit of the two coupled rectangular microstrip patch antennas.

The two coupled rectangular microstrip patch antennas shown in Fig.3 is represented by an equivalent transmission line model as shown in Fig.4. In Fig.4, the radiation admittance Y= G+jωC of the rectangular microstrip patch antenna is composed of a parallel combination of the radiation conductance G and the capacitance C given by Hong et al.[14]. Here ω is the angular frequency. The REC model is composed of a conductance and the capacitances. This conductance is given by the radiation conductance of the rectangular microstrip patch antenna and these capacitances are determined from the unnormalized series and shunt susceptances. Y_o is the characteristic admittance of the microstrip patch[16]. X_L is the inductive reactance of a coaxial feed and is given by[17]

$$X_L = \frac{\eta_o}{\sqrt{\epsilon_r}} \tan\left(\frac{2\pi h}{\lambda_o}\right) \tag{1}$$

where η_o is the intrinsic impedance in the free space, and λ_o is the free space wavelength.

The equivalent radiation admittance Y_1 is expressed as

$$Y_1 = Y_o \frac{Y + j\ Y_o\ \tan\beta X}{Y_o + j\ Y\ \tan\beta X} \tag{2}$$

where $\beta = \frac{2\pi}{\lambda_o}\sqrt{\epsilon_{eff}}$ is the propagation constant of the transmission line and ϵ_{eff} is the effective dielectric constant[16]

The equivalent circuit shown in Fig.4 represents a 2-port network. The entire 2-port transmission matrix representation [T] is found by cascading nine successional transmission matrices from port 1 to port 2 given by

$$\begin{bmatrix} T_{11} & T_{12} \\ T_{21} & T_{22} \end{bmatrix} = [T_{X_L}]\,[T_{Y_1}]\,[T_{L-X}]\,[T_{sh}]\,[T_s]\,[T_{sh}]\,[T_{L-X}]\,[T_{Y_1}]\,[T_{X_L}] \tag{3}$$

where $[T_{X_L}]$ represents the transmission matrix of the inductive reactance element. $[T_{Y_1}]$ and $[T_{L-X}]$ represent the equivalent radiation admittance matrix and transmission line (L-X) matrix, respectively. $[T_{sh}]$ and $[T_s]$ represent the shunt and series elements matrices of the REC model, respectively.

Each transmission matrix is expressed as follows:

$$[T_{X_L}] = \begin{bmatrix} 1 & jX_L \\ 0 & 1 \end{bmatrix} \tag{4a}$$

$$[T_{Y_1}] = \begin{bmatrix} 1 & 0 \\ Y_1 & 1 \end{bmatrix} \tag{4b}$$

$$[T_{L-X}] = \begin{bmatrix} \cos\beta(L-X) & j\frac{1}{Y_o}\sin\beta(L-X) \\ jY_o\sin\beta(L-X) & \cos\beta(L-X) \end{bmatrix} \tag{4c}$$

$$[T_{sh}] = \begin{bmatrix} 1 & 0 \\ j\omega C_{sh} & 1 \end{bmatrix} \tag{4d}$$

$$[T_s] = \begin{bmatrix} 1 & \frac{1}{G + j\omega C_s} \\ 0 & 1 \end{bmatrix} \tag{4e}$$

Impedance matrix [Z] can be obtained by transforming the entire transmission matrix elements given in (3) as follows:

$$\begin{bmatrix} Z_{11} & Z_{12} \\ Z_{21} & Z_{22} \end{bmatrix} = \begin{bmatrix} \frac{T_{11}}{T_{21}} & \frac{T_{11}T_{22}}{T_{21}} - T_{12} \\ \frac{1}{T_{21}} & \frac{T_{22}}{T_{21}} \end{bmatrix} \tag{5}$$

Scattering matrix [S] which characterizes the two rectangular microstrip patch antennas which are coupled to the radiating edges between the patches can be obtained by transforming the impedance matrix elements as follows:

$$\begin{bmatrix} S_{11} & S_{12} \\ S_{21} & S_{22} \end{bmatrix} = \begin{bmatrix} \frac{(\bar{Z}_{11}-1)(\bar{Z}_{22}+1) - \bar{Z}_{12}\bar{Z}_{21}}{\triangle} & \frac{2\bar{Z}_{12}}{\triangle} \\ \frac{2\bar{Z}_{21}}{\triangle} & \frac{(\bar{Z}_{11}+1)(\bar{Z}_{22}-1) - \bar{Z}_{12}\bar{Z}_{21}}{\triangle} \end{bmatrix} \tag{6}$$

Where

$$\bar{Z}_{ij} = \frac{Z_{ij}}{50} \quad (i,\ j = 1, 2)$$

$$\triangle = (\bar{Z}_{11}+1)(\bar{Z}_{22}+1) - \bar{Z}_{12}\bar{Z}_{21}$$

Because the equivalent circuit shown in Fig.4 is symmetrical, $S_{11} = S_{22}$ and $S_{12} = S_{21}$. Here S_{ii} is signified as the reflection coefficient at the ith port with the jth port matched to a 50-Ω load. The S_{ij} is signified as the transmission coefficient which flows from jth port to ith port when the jth port is matched to a 50-Ω load.

The antenna specifications are listed in Table 1, Here, X means a 50-Ω feed point location whose the input impedance of the rectangular microstrip patch antenna is equal to 50 Ω. X is 0.894cm[14].

For the antenna given in Table 1, we calculate the series and shunt capacitances of the REC

Table 1. Specifications of two coupled rectangular microstrip patch antennas.

Patch Length L [cm]	Patch Width W [cm]	Substrate Thickness h [cm]	Dielectric Constant ϵ_r	Feed Point X [cm]
3.02	3.7	0.155	2.6	0.894

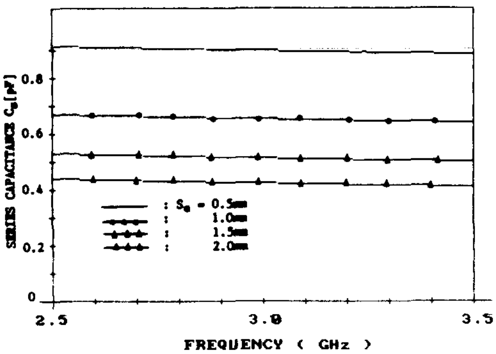

Fig.5. Calculated series capacitances C_S of the REC model as a function of frequency for the various coupling separations.

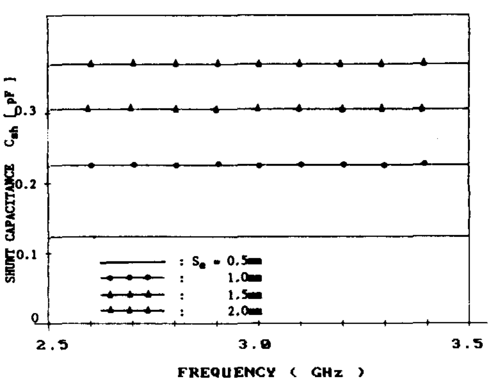

Fig.6. Calculated shunt capacitances C_{sh} of the REC model as a function of frequency for the various coupling separations.

model for the cases of coupling separation S_e = 0.5mm, 1.0mm, 1.5mm, and 2.0mm.

Fig.5 and 6 show the calculated series and shunt capacitances (C_S and C_{sh}) of the REC model, respectively, as a function of frequency for the four coupling separations. As mentioned in Section II, it is also observed that the series capacitance C_S increases and the shunt capacitance C_{sh} decreases with decreasing the coupling separation S_e.

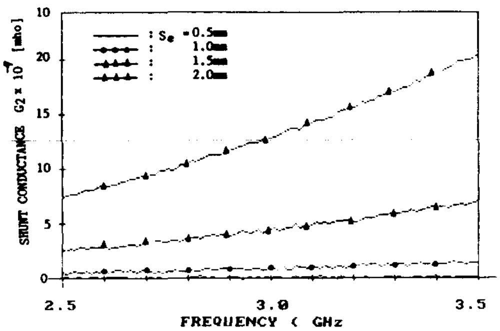

Fig.7. Calculated shunt conductances G_2 of the equivalent circuit for the geometry in Fig.2(a) for the various coupling separations.

When the slit width 2a is equal to the coupling separation Se, the unnormalized shunt conductances G_2 of the equivalent circuit for the geometry in Fig.2(a) are calculated and plotted as a function of frequency in Fig.7 for the cases of S_e=0.5mm, 1.0mm, 1.5mm, and 2.0mm. It is evident from Fig.7 that for the various coupling separations, the shunt conductances of the equivalent circuit become extremely small. Therefore, as mentioned in Section II, the shunt conductance is neglected so that the shunt element of the REC model is only composed of the shunt capacitance Csh.

Applying the REC model and the radiation admittance in the two coupled rectangular microstrip patch antennas, we obtain numerical scattering parameter results of $|S_{11}|$ and $|S_{12}|$ for the various coupling separatios. Fig.8 and 9 show the values of $|S_{11}|$ and $|S_{12}|$ as a function of frequency for the four coupling separations, S_e=0.5, 1.0, 1.5, and 2.0 mm. It is observed in Fig.8 that as the coupling separation increases, the swelling diminishes slighter, the Dip becomes sharper, and the Dip frequency shifts lower. From the trend of the curves, when the coupling separation is sufficiently increased, the coupling is nearly neglected so that the two coupled

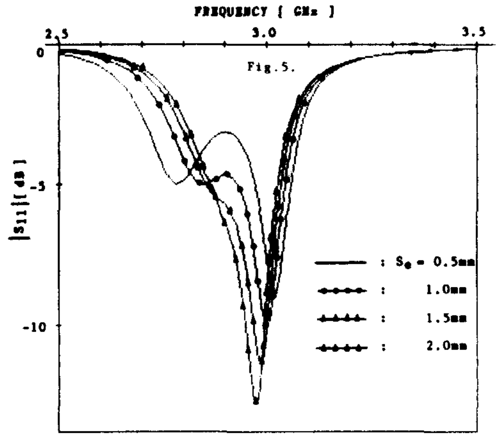

Fig.8. Numerical results of $|S_{11}|$ as a function of frequency for the various coupling separations, S_e=0.5, 1.0, 1.5, and 2.0mm.

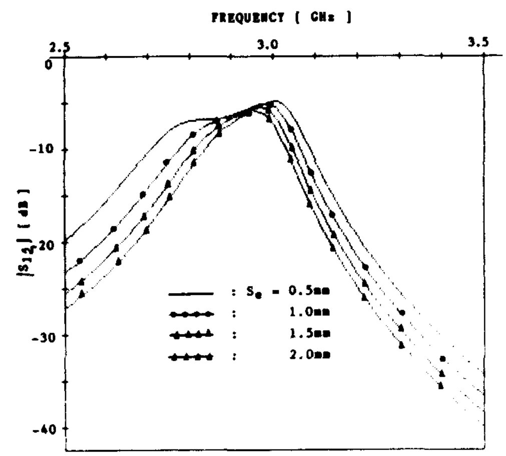

Fig.9. Numerical results of $|S_{12}|$ as a function of frequency for the various coupling separations, S_e=0.5 1,0, 1,5, and 2.0mm.

rectangular microstrip patch antennas are operated independently as an isolated rectangular microstrip patch antenna, respectively. In this case, i.e., for the completely uncoupled case, the Dip frequency approaches the resonant frequency 2.910GHz which is calculated by the single rectangular microstrip patch antenna given by Hong et al. [14].

The calculated values of $|S_{12}|$ for the various coupling separations are illustrated in Fig.9. It is observed that the calculated values of $|S_{12}|$ decrease with increasing the coupling separation. This effect is easily deduced by directly inspecting Fig.8.

In order to provide a comparision of the REC model presented in this paper with previous E-plane coupling model, the equivalent circuit for the two coupled rectangular microstrip patch antennas described by Krowne[7] is shown in Fig.10.

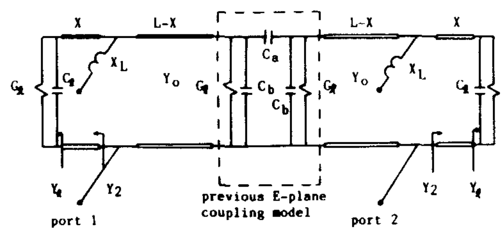

Fig.10. Equivalent circuit of previous E-plane coupling model proposed by krowne[7].

As seen in Fig.10, the previous E-plane coupling model is entirely different from the REC model. The previous E-plane coupling model is composed of an equivalent circuit proposed by Maeda[6] and two identical conductances. The series and shunt gap capacitances (C_a and C_b) of the equivalent circuit, are calculated by using a quasi-static variational approach. The two identical conductances are given by a radiation conductance of the rectangular microstrip patch antenna. The radiation admittance $Y_\ell=G_\ell+jwC_\ell$ is composed of a radiation conductance G_ℓ and a capacitance C_ℓ. Here, Krowne used the aperture conductance for a flanged parallel-plate waveguide into a half space analyzed by Harrington[18] as the radiation conductance, and a capacitance expressed by function of the line extension[19] as the radiation capacitance.

As shown in Fig.10, for the equivalent circuit described by Krowne[7], the total transmission matrix [T'] is expressed as

$$\begin{bmatrix} T'_{11} & T'_{12} \\ T'_{21} & T'_{22} \end{bmatrix} = [T_{X_L}][T_{Y_2}][T_{L-X}][T_b][T_a][T_b][T_{L-X}][T_{Y_2}][T_{X_L}] \quad (7)$$

where

$$[T_{Y_2}] = \begin{bmatrix} 1 & 0 \\ Y_2 & 1 \end{bmatrix}$$

$$[T_b] = \begin{bmatrix} 1 & 0 \\ G_l + j\omega C_b & 1 \end{bmatrix}$$

$$[T_a] = \begin{bmatrix} 1 & \dfrac{1}{j\omega C_a} \\ 0 & 1 \end{bmatrix}$$

$$Y_2 = Y_o \frac{Y_l + j\ Y_o \tan\beta X}{Y_o + j\ Y_l \tan\beta X}$$

$$Y_l = G_l + j\,\omega\, C_l$$

$$G_l = \frac{\pi W}{\lambda_o \eta_o}\left[1 - \frac{(kh)^2}{24}\right]$$

$$C_l = \frac{Y_o}{v_p} \cdot 0.412 \cdot h \cdot \frac{\epsilon_{eff} + 0.3}{\epsilon_{eff} - 0.258} \cdot \frac{W/h + 0.262}{W/h + 0.813}$$

and v_p is the phase velocity of the microstrip patch.

For the previous E-plane coupling model, theoretical values of $|S_{11}|$ and $|S_{12}|$ are obtained by transforming the transmission and impedance matrix elements as given in (5) and (6), respectively.

Table 2. Comparision of the series and shunt capacitances of the REC model with the series and shunt gap capacitances of the previous E-plane model.

Coupling Separation S_e (mm)	Series Capacitance (pF)		Shunt Capacitance (pF)	
	REC model C_s	Previous model C_a	REC model C_{sh}	Previous model C_b
0.5	0.9182	1.2885	0.1248	0.1263
1.0	0.6688	1.0186	0.2262	0.2315
1.5	0.5315	0.8302	0.3070	0.3412
2.0	0.4416	0.7122	0.3709	0.4274

A comparision of the series and shunt capacitances (C_s and C_{sh}) of the REC model with the series and shunt gap capacitances (C_a and C_b) of the previous E-plane coupling model is given in Table 2. The series and shunt capacitances (C_s, C_{sh}) given in Table 2 are the maximum values in the frequency range of 2.5-3.5 GHz because these values slightly vary with frequency, as shown in Fig.5 and 6. It is seen from Table 2 that for each coupling separation, the values of C_s are smaller than those of C_a, and the values of C_{sh} are nearly the same as those of C_b.

IV. Experimental Results and Discussion

For the cases of S_e=0.5, 1.0, 1.5 and 2.0 mm, experimental values of $|S_{11}|$ and $|S_{12}|$ are compared with theoretical results. The two coupled rectangular microstrip patch antennas are fabricated in Teflon substrate with relative dielectric constant ϵ_r=2.6 and thickness h=0.155cm. Measurements are carried out in the frequency range of 2.5-3.5 GHz with HP-8746B S-parameter Test Set.

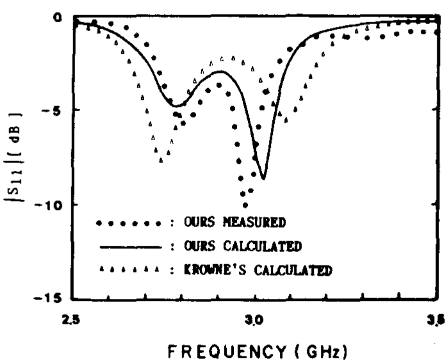

(a) $|S_{11}|$

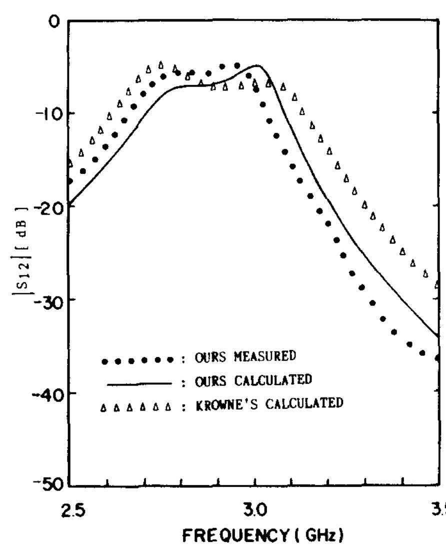

(b) $|S_{12}|$

Fig.11. Measured and calculated S-parameter values as a function of frequency for S_e= 0.5mm.

The calculated and measured values of $|S_{11}|$ and $|S_{12}|$ for the cases of S_e=0.5, 1.0, 1.5 and 2.0 mm, are shown as a function of frequency in Figs. 11-14. In Fig.11(a) and (b), for S_e= 0.5mm, the measured and calculated values of $|S_{11}|$ and $|S_{12}|$ obtained by the REC model are illustrated and compared with theoretical results obtained by the previous E-plane coupling model[7]. It is worth while to point out in Fig.11(a) and (b) that the measured values are more in agreement with our calculasted results than the calculated results obtained by the equivalent circuit of Krowne[7]. As shown in Fig.11(a) and (b), the small shift in the Dip frequency may be due to the fact that the frequency discrepancy between the calculated and measured resonant frequency was occured in the rectangular microstrip patch antenna.

The calculated and measured values of $|S_{11}|$ and $|S_{12}|$ for the three coupling separations, S_e=1.0, 1.5, and 2.0 mm are illustrated in Figs.12-14. It is also observed from Figs.12-14 that the measured values are in agreement with the calculated results obtained from the REC model.

As discussed in Section II, it is also observed from the meansured results in Figs.11-14 that the swelling diminishes progressively and the Dip frequency shifts lower with increasing the

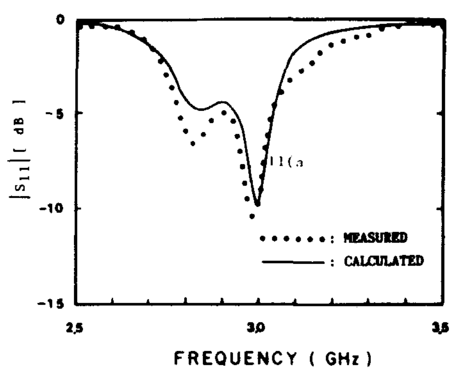

(a) $|S_{11}|$

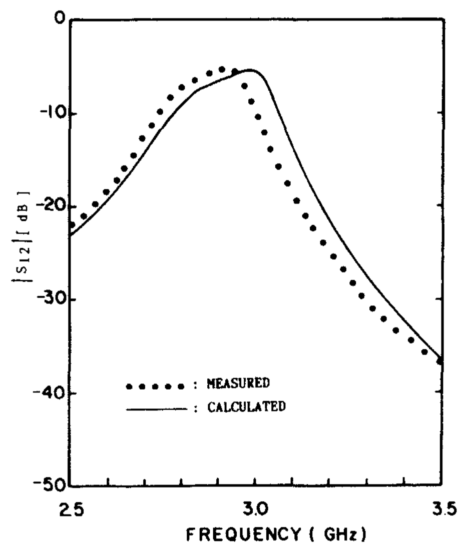

(b) $|S_{12}|$

Fig.12. Measured and calculated S-parameter values as a function of frequency for S_e=1.0mm.

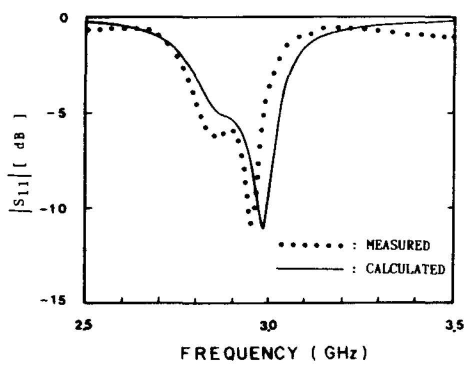

(a) $|S_{11}|$

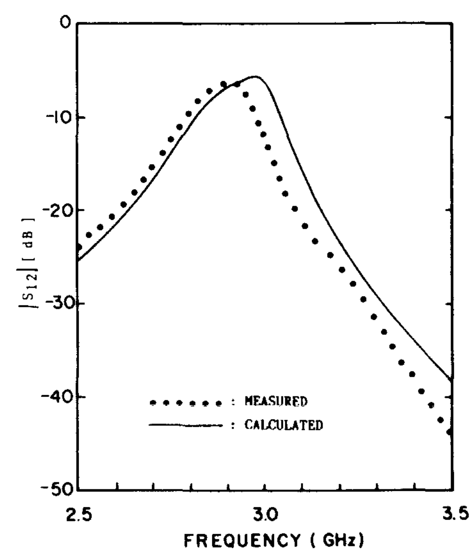

(b) $|S_{12}|$

Fig.13. Measured and calculated S-parameter values as a function of frequency for S_e= 1.5mm.

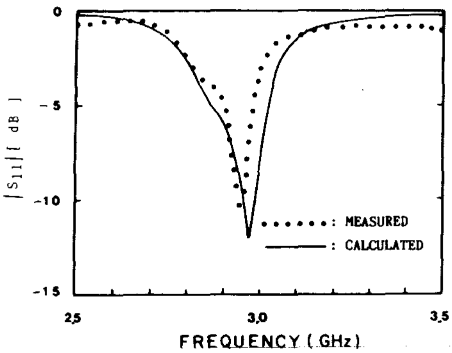

(a) $|S_{11}|$

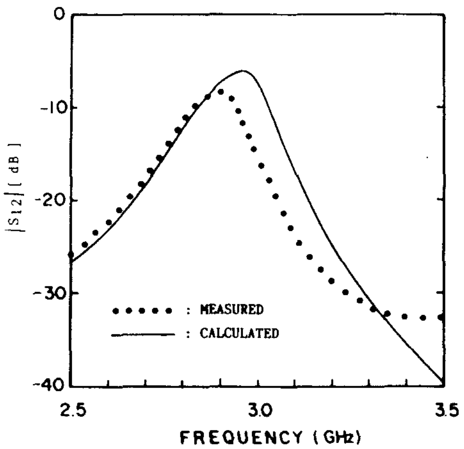

(b) $|S_{12}|$

Fig.14. Measured and calculated S-parameter values as a function of frequency for S_e=2.0mm.

coupling separation. From Figs.11-14, we can conclude that when coupling separation is sufficiently increased, $|S_{11}|$ is interpreted physically as the return loss of the single rectangular microstrip patch antenna. In this case, the Dip frequency approaches the resonant frequency fo=2.910 GHz given by Hong et al.[14].

V. Conclusion

A new model is presented which characterizes the coupling of the radiating edges between two rectangular microstrip patch antennas. This model, namely Radiating Edges-Coupling (REC) model, is derived from the equivalent circuit of the slitted parallel-plate waveguide filled with homogeneous dielectric.

Applying the REC model presented here and the radiation admittance given by Hong et al.[14] to two coupled rectangular microstrip patch antennas, we obtained numerical S-parameter values of $|S_{11}|$ and $|S_{12}|$ for the various coupling separations, S_e=0.5, 1.0, 1.5, and 2.0 mm. Experiments are performed in the frequency range of 2.5-3.5 GHz. The antennas are fabricated in Teflon substrate with relative dielectric constant ϵ_r=2.6 and thickness h=0.155cm. We observed that theoretical values are in fairly good agreement with experimental results. Further, it is concluded that the REC model is more accurate than the previous E-plane model by Krowne[7]. From the measured and calculated results, we can deduce that when the coupling separation is sufficiently increased, $|S_{11}|$ of the two coupled rectangular microstrip patch antennas is interpreted physically as the return loss of the single rectangular microstrip patch antenna.

The REC model presented in this paper is very valuable for the design of rectangular microstrip patch array antenna[20] and for the bandwidth broadening techniques.

References

[1] C.K. Aanadan and K.G. Nair, "Compact broadband microstrip antenna," *Elect. Letters*, vol. 22, no. 20, pp. 1064-1065, Sept. 1986.

[2] H. Entschladen and U. Nagel, "Microstrip patch array antennas," *Elect. Letters,* vol. 20, pp. 931-933, 1983.

[3] C. Wood, "Improved bandwidth of microstrip antennas using parasitic elements," *IEE Proc. H, Microwaves, Opt. & Antennas,* vol. 127, no. 4, pp. 231-234, Aug. 1980.

[4] G. Kumar and K.C. Gupta, "Broad-band microstrip antennas using additional resonators gap-coupled to the radiating edges," *IEEE Trans. Antennas Propagat.,* vol. AP-32, no. 12, pp. 1375-1379, Dec. 1984.

[5] G. Kumar and K.C. Gupta, "Nonradiating edges and four edges gap-coupled multiple resonator broad-band microstrip antennas," *IEEE Trans. Antennas Propagat* vol. AP-33, no. 2, pp. 173-178, Feb. 1985.

[6] M. Maeda, "An analysis of gap in microstrip transmission lines," *IEEE Microwave Theory Tech.*, vol. MTT-20, pp. 390-395, June 1927.

[7] C.M. Krowne, "E-plane coupling between two rectangular microstrip antennas," *Elect. Letters*, vol. 16, no. 16, pp. 635-636, July 1980.

[8] C.M. Krowne, "Dielectric and width effect on H-plane and E-plane coupling between rectangular microstrip antennas," *IEEE Trans. Antennas Propagat.*, vol. AP-31, no. 1, pp. 39-47, Jan. 1983.

[9] R.Q. Lee, R. Acosta, and K.F. Lee, "Radiation characteristics of microstrip arrays with parasitic elements," *Elect. Letters*, vol. 23, no. 16, pp. 835-837, July 1987.

[10] K. Özmehmet, "New frequency dependent equivalent circuit for gap discontinuities of microstriplines," *IEE Proc. H, Microwaves, Opt. & Antennas*, vol. 134, no. 3, pp. 333-335, June 1987.

[11] Young Ki Cho, "On the equivalent circuit representation of the slitted parallel-plate waveguide filled with a dielectric," to be published *IEEE Trans. Antennas Propagat., in future issue.*

[12] Seung Gak Kim and Young Ki Cho et al., "Equivalent circuit description for a parallel-plate waveguide with a transverse slit in its upper plate," *Journal of KITE*, vol. 25, no. 4, pp. 11-16, Apr. 1988.

[13] Jae Pyo Hong, Young Ki Cho, and Hyon Son, "Analysis of the rectangular microstrip antenna with parasitic element," *KITE conference at Kyunghee University in Soowon*, pp. 433-434, July 1988.

[14] Jae Pyo Hong, Young Ki Cho, and Hyon Son, "Improved method for calculating radiation admittance of a rectangular microstrip patch antenna," *Journal of KITE*, vol. 26, no. 2, Feb. 1989.

[15] I.J. Bahl, "Build microstrip antennas paper-thin dimensions," Microwaves, vol. 18, pp. 50-63, Oct. 1979.

[16] D.L. Sengupta, "Approximate expression for the resonant frequency of a rectangular patch antenna, " *Elect. Letters*, vol. 19, no. 20, pp. 834-835, Sept. 1983.

[17] K.R. Carver, "Practical analytical techniques for the microstrip antenna," Proc. Workshop on Printed Circuit Antennas, New Mexico State University, pp. 7.1-7.20, Oct. 1979.

[18] R.F. Harrington, Time-Harmonic Electromagnetic Fields, New York: McGraw-Hill, 1961.

[19] A.G. Derneryd, "Lineary polarized microstrip antennas," *IEEE Trans. Antennas Propagat.*, vol. AP-24, no. 6, pp. 846-851, Nov. 1976.

[20] Jae Pyo Hong, Young Ki Cho, and Hyon Son, "Input impedance of rectangular microstrip antenna array using E-plane coupling"' *KITE conference at Konkuk University in Seoul,* vol. 11, no. 11, pp. 163-165, Nov. 1988. *

著 者 紹 介

洪 在 杓 (正會員) 第26巻 第2號 參照
현재 순천공업전문대학 전자과 전임강사.

趙 榮 基 (正會員) 第26巻 第2號 參照
현재 경북대학교 전자공학과 조교수.

孫 鉉 (正會員) 第26巻 第2號 參照
현재 경북대학교 전자공학과 재직중.